Gaussian Pulse Characterization of RF Power Amplifiers

Tommaso Cappello, *Member, IEEE*, Zoya Popovic, *Fellow, IEEE*, Kevin Morris, *Member, IEEE*, and Angelo Cappello

Abstract—This work presents a new RF power amplifier characterization technique based on a Gaussian pulse, which is shown to approximate the envelope of a multicarrier signal with 0.5% error around the peaks. The standard deviation of the Gaussian pulses is inversely proportional to the I/Q signal bandwidth. This test signal is shown to accurately capture nonlinear memory effects that result in gain dispersion after the peak power is reached. As an example, it is shown that the gain amplitude and phase can vary up to 2.3 dB and 6° for a 10-W 3.75-GHz GaN power-amplifier evaluation board, depending on the I/Q signal bandwidth and peak power level.

Index Terms—Gallium nitride, memory effects, nonlinear characterization, power amplifier (PA), RF measurements, trapping effects.
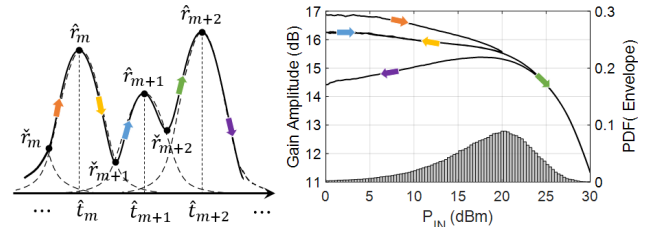

Fig. 1.   Left: Multicarrier signal envelope (solid line) approximated by a train of amplitude-scaled time-shifted Gaussian pulses (dashed line). Right: PA gain with colored arrows highlighting the gain variation caused by the envelope peaks. The PDF of the entire envelope is also shown to highlight the impact of backoff gain dispersion.

I. INTRODUCTION

BEHAVIORAL modeling of RF power amplifiers (PAs) relies on characterization with test signals capable of exciting nonlinear memory effects accounted by the model [1]. These effects are mainly caused by matching and biasing circuits, transistor parasitics, temperature, and in some technologies (e.g., GaAs or GaN) by charge-trapping phenomena [2]–[5]. Memory time constants are in the ns to s range, affecting a wide spectrum response of the PA, from a few hertz to gigahertz from the carrier frequency [6]. Nonlinear memory effects are more detrimental when amplifying signals with large peak-to-average power ratios (PAPRs), such as in multicarrier signals. A (local) maximum of the envelope temporarily changes the PA behavior, and if the envelope remains below this value, the PA can recover to a certain degree [5]. This is illustrated in Fig. 1 with the colored arrows.

Test signals used in PA behavioral modeling include: 1) the application signal itself (e.g., LTE); 2) single-, two-, or multitone sinusoidal signals [7]–[9]; and 3) single, double, or multiple pulses [10]–[12]. The first approach leads to signal-dependent PA gain characterization; when the signal changes, the characterization data are no longer representative of the PA behavior. The other two approaches are more general

and the main differentiator is their time-frequency resolution: multitone test signals enable the study of precisely located effects in the frequency domain but they require a large number of tones to capture both slow and fast effects [9]. Rectangular pulses allow instead the study of precisely located effects in time domain if a fast rise and fall time is used, but they result in a unnecessarily broadband PA excitation (with possible ringing).

In this work, we propose a new characterization technique using a Gaussian pulse which optimizes the time-frequency resolution of the characterization based on the signal application: the rise and fall times of the Gaussian waveform closely match those of the multicarrier test signal, or equivalently the spectral response of a Gaussian pulse approximates the bandwidth of the application signal. This technique also simplifies the PA characterization by avoiding the use of a high number of rectangular pulses or sinusoidal tones as only a single Gaussian pulse is required to extract the PA characteristic. This approach is similar to other hybrid time-frequency analysis techniques such as Wavelet transform. However, Gaussian pulses are appropriate due to the stationary nature of the signal [13] and the sensitivity of a RF-PA to voltage peaks.

II. GAUSSIAN CHARACTERIZATION

Multicarrier signals (e.g., downlink LTE [14]) are commonly used in high-capacity wireless links. A bit stream is split into N lower-rate symbol streams x_n, which are modulated by N subcarriers with frequency spacing $1/T$

$$x(t) = i(t) + jq(t) = \sum_{n=1}^{N} x_n e^{j2\pi nt/T}. \tag{1}$$

Here T is the signal period, and symbols x_n belong to an independent identically distributed random variable X [15]. For large N, because of the central limit theorem (CLT) [16],

This article has been accepted for inclusion in a future issue of this journal. Content is final as presented, with the exception of pagination.

2   IEEE MICROWAVE AND WIRELESS COMPONENTS LETTERS
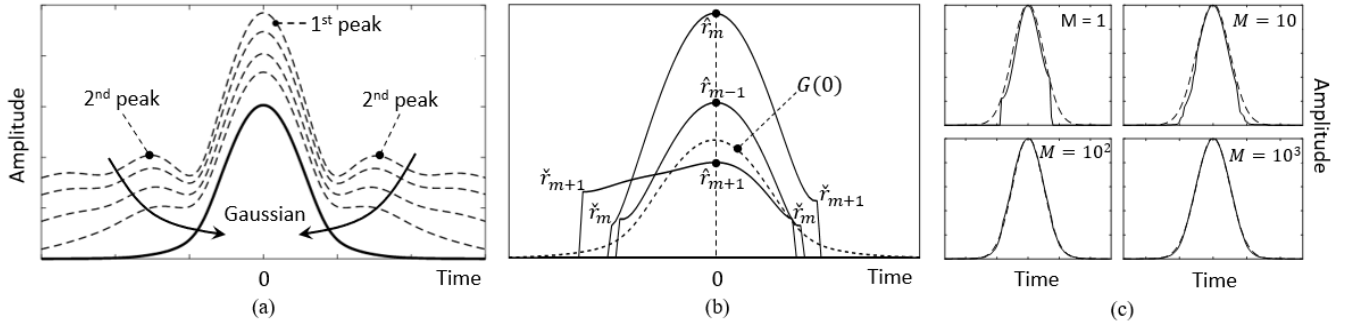
Fig. 2. (a) Application of the algorithm to partitions of different durations: when the partition is delimited by two consecutive minima, the minima–maxima algorithm converges to a bell-shaped pulse which can be approximated with 99.5% confidence by a Gaussian waveform (solid line); for longer partitions, the tail of the curve presents a second peak (dashed line). (b) Envelope partitioning and time alignment between several pulses, and resulting Gaussian waveform (dashed line). (c) Average (solid line) of an increasing number M of partitions approaches a Gaussian (dashed line).

the real and imaginary parts of X tend to a Gaussian distribution with zero mean and standard deviation σ, namely

$$I \sim \frac{1}{\sqrt{2\pi\sigma^2}}\exp\left(\frac{-i^2}{2\sigma^2}\right), \quad Q \sim \frac{1}{\sqrt{2\pi\sigma^2}}\exp\left(\frac{-q^2}{2\sigma^2}\right). \quad (2)$$

It is widely accepted the PA nonlinear memory effects are caused by signal amplitude as described by AM–AM and AM–phase modulation (PM) model, therefore, X is expressed in polar form

$$R \sim \frac{r}{\sigma^2}\exp\left(\frac{-r^2}{2\sigma^2}\right), \quad \Theta \sim \begin{cases} 1/2\pi, & -\pi \leq \theta < \pi \\ 0, & \text{otherwise.} \end{cases} \quad (3)$$

A numerical representation of random variable R is given in Fig. 1 where it is seen that its shape tends to a Rayleigh probability density function (PDF) (note the logarithmic scale). Equation (3), however, does not provide information on amplitude distribution, or if a recurring shape is present in the envelope.

In this work, we aim to extract the most likely repetitive shape in a multicarrier signal envelope, and to this purpose we average the multicarrier envelope pulses to find a recurring waveform. A rigorous proof is outside the scope of this letter, and here we provide a numerical demonstration that a bell-shaped pulse gives the desired approximation of the envelope. This result can be possibly justified by the CLT as a large number of pulses are required to obtain a shape that can be approximated with 99.5% confidence by a Gaussian waveform.

The minima–maxima decomposition algorithm can be summarized as follows.

1) The envelope is partitioned based on consecutive minima. The mth partition is delimited by two consecutive minima $\check{t}_m$ and $\check{t}_{m+1}$, namely

$$P_m = [r(\check{t}_m), \ldots, r(\hat{t}_m), \ldots, r(\check{t}_{m+1})]. \quad (4)$$

As seen in Fig. 2(a), if the envelope partitions include more than one maximum (or more than two minima), their average presents a second peak (dashed lines). When instead the partition is defined by two nearest minima, the average tends to a Gaussian pulse with 99.5% R-square confidence.

2) From Rolle's theorem, a maximum $r(\hat{t}_m)$ is present between two consecutive minima, so the maximum $\hat{r}_m$ can be aligned to $t = 0$ as also qualitatively depicted in Fig. 2(b).
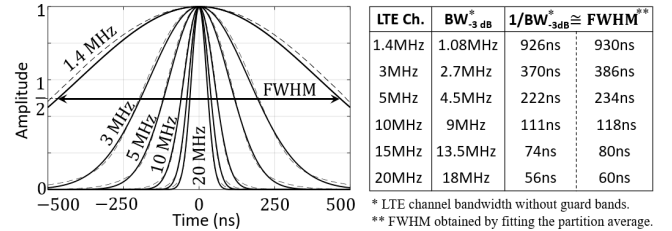

Fig. 3. Bell-shaped curves (dashed line) resulting from the application of the algorithm and fitting with Gaussian waveforms (solid line). Table: LTE channel bandwidths and corresponding Gaussian FWHM duration which is approximately equal to the $1/\text{BW}_{-3\text{ dB}}$.

LTE Ch.	BW*$_{-3\text{ dB}}$	1/BW*$_{-3\text{dB}} \cong$ FWHM**
1.4MHz	1.08MHz	926ns	930ns
3MHz	2.7MHz	370ns	386ns
5MHz	4.5MHz	222ns	234ns
10MHz	9MHz	111ns	118ns
15MHz	13.5MHz	74ns	80ns
20MHz	18MHz	56ns	60ns

* LTE channel bandwidth without guard bands.
** FWHM obtained by fitting the partition average.

3) The average of a large-enough number M of partitions tends to a bell-shaped curve [Fig. 2(c)] which can be approximated by a Gaussian waveform with standard deviation τ and maximum value $\bar{r}(0)$, namely

$$P_{\text{avg}} = \frac{1}{M}\sum_{m=1}^{M} P_m \approx G(0) = \bar{r}(0)\exp\left(\frac{-t^2}{2\tau^2}\right). \quad (5)$$

It is interesting to note the similarity between (5) obtained by minima–maxima analysis in the time domain and the original I/Q amplitude PDF of (2). The full-width at half-maximum (FWHM) of a Gaussian pulse in time domain is

$$\text{FWHM} = \sqrt{8\ln 2}\cdot\tau \cong 2.355\cdot\tau. \quad (6)$$

The FWHM is also inversely proportional to the I/Q signal bandwidth $\text{BW}_{-3\text{ dB}}$ as verified in table of Fig. 3. Therefore

$$\text{FWHM} \approx \frac{1}{\text{BW}_{-3\text{ dB}}} \quad \rightarrow \quad \tau \cong \frac{1}{2.355\cdot\text{BW}_{-3\text{ dB}}}. \quad (7)$$

In summary, this last property can be used to investigate the PA behavior in response to an arbitrary I/Q signal with −3 dB bandwidth equal to 1/FWHM.

III. EXPERIMENTAL RESULTS

This characterization technique is validated with an evaluation board of a Wolfspeed CG2H40010F GaN-on-SiC transistor. The PA input and output signals are sensed with couplers connected to a 200-MHz vector signal generator and analyzer (NI PXIe-5646R VST) as shown in Fig. 4. Power calibration is performed at 3.75 GHz (PA central frequency). Six LTE signals with channel bandwidths of 1.4, 3, 5, 10, 15, and 20 MHz are generated according to the E-UTRA FDD test
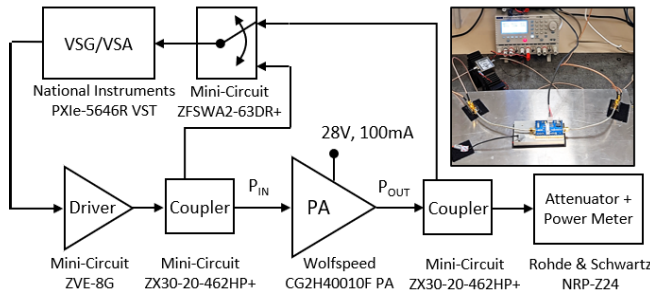
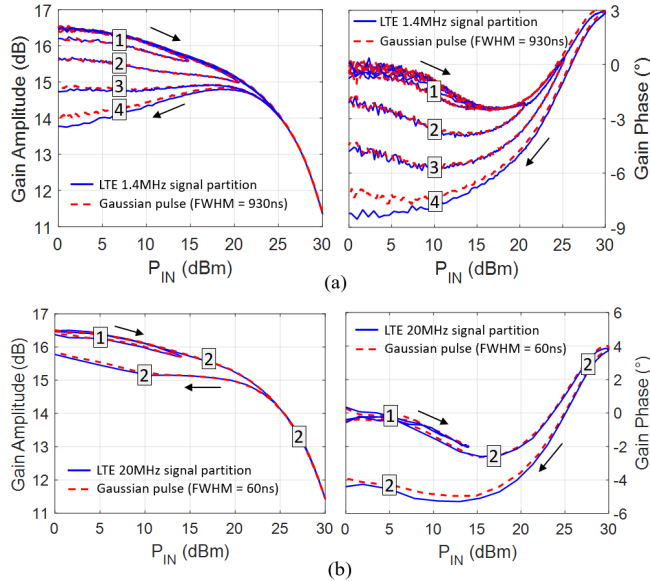Fig. 4. Block diagram and photograph of the setup.

Fig. 5. Experimental validation of the Gaussian characterization technique: the PA gain extracted with random time-partitions of (a) 1.4 MHz and (b) 20 MHz LTE signal with varying amplitudes is compared with the gain extracted with a Gaussian pulse. The gain characteristics obtained with the Gaussian pulse match the ones obtained with the LTE partitions.
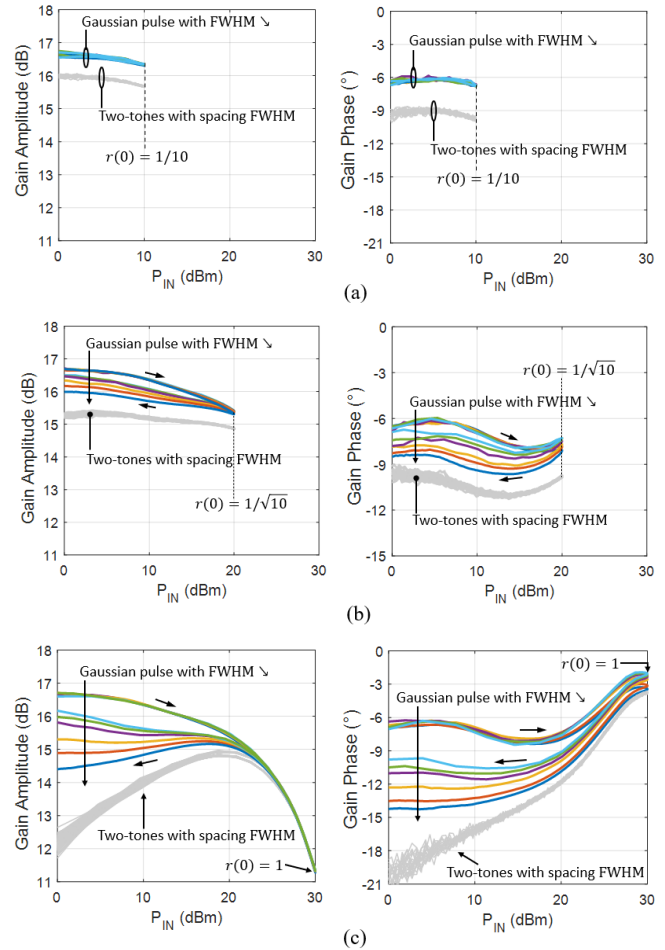

Fig. 6. PA gain and phase obtained with a Gaussian pulse with (a) $r(0) = 1/10$, (b) $r(0) = 1/\sqrt{10}$, and (c) $r(0) = 1$. Two-tone characterization with spacing equal to the FWHM of the Gaussian pulse are also reported to highlight the inadequacy of this test, especially in backoff.

model (v1.1) and are used as a benchmark for the validation of the technique. We note that the -3 dB bandwidths of these LTE signals is obtained by removing the guard bands and results in the values in the second column of the table in Fig. 3.

The Gaussian characterization technique is validated against partitions of the original LTE signal with the aim of showing the equivalence between the two waveforms in capturing the PA gain. Fig. 5(a) reports the gain resulting from four random partitions at increasing amplitudes of the 1.4-MHz LTE signal, extracted with the algorithm of Section II, which are compared to the PA gain in response to a Gaussian pulse with FWHM = 930 ns. The two techniques provide very similar results both in gain amplitude and phase. Similarly, the gain resulting from a 20-MHz LTE signal excitation is compared to a Gaussian pulse with FWHM = 60 ns showing good agreement, Fig. 5(b).

Next, the flexibility of the characterization technique is demonstrated by measuring the gain of the PA for all the LTE signal bandwidths, Fig. 6. The gain amplitude and phase is approximately the same until it reaches the peak output power ($\rightarrow$ direction). For $r(0) = [1/\sqrt{10}, 1]$, the gain after the maxima is degraded to a lower amplitude and phase value ($\leftarrow$ direction). For lower LTE bandwidths, this dispersion is larger, possibly because of a longer pulse duration (higher self-heating) and permanence at higher voltage levels

(more charge trapping). It is noted that this gain and phase dispersion occurs for envelope amplitudes well below 10 dB which represent 71%–77% of the entire signal duration (see PDF on Fig. 1), and this justifies the need for a flexible signal representation capable of capturing these effects within the signal evolution.

IV. Conclusion

In this letter, we present a novel characterization technique based on a Gaussian waveform suitable for studying the nonlinear memory effects in RF PAs. A minima–maxima algorithm is used to extract the most-likely pulse shape within a multicarrier signal, which can be approximated by a Gaussian pulse, with FWHM inversely proportional to the I/Q signal bandwidth. The Gaussian pulse and the original "LTE pulse" are demonstrated to be equivalent in extracting the PA characteristics. This technique is then applied to characterize the gain of the PA with a Gaussian-pulse instead of a 1.4–20 MHz LTE signal, which results in a gain and phase deviations of up to 2.3 dB and 6°, respectively.

REFERENCES

[1] J. Wood, *Behavioral Modeling and Linearization of RF Power Amplifiers* (Artech House Microwave Library). Norwood, MA, USA: Artech House, 2014. [Online]. Available: https://books.google.it/books?id=abpTBAAAQBAJ

[2] G. P. Gibiino, T. Cappello, D. Niessen, D. M. M.-P. Schreurs, A. Santarelli, and F. Filicori, "An empirical behavioral model for RF PAs including self-heating," in *Proc. Integr. Nonlinear Microw. Millimetre-Wave Circuits Workshop (INMMiC)*, Oct. 2015, pp. 1–3.

[3] V. Camarchia, F. Cappelluti, M. Pirola, S. D. Guerrieri, and G. Ghione, "Self-consistent electrothermal modeling of class A, AB, and B power GaN HEMTs under modulated RF excitation," *IEEE Trans. Microw. Theory Techn.*, vol. 55, no. 9, pp. 1824–1831, Sep. 2007.

[4] F. Filicori, G. Vannini, A. Santarelli, A. M. Sanchez, A. Tazon, and Y. Newport, "Empirical modeling of low-frequency dispersive effects due to traps and thermal phenomena in III-V FET's," *IEEE Trans. Microw. Theory Techn.*, vol. 43, no. 12, pp. 2972–2981, Dec. 1995.

[5] T. Cappello, C. Florian, A. Santarelli, and Z. Popovic, "Linearization of a 500-W L-band GaN Doherty power amplifier by dual-pulse trap characterization," in *IEEE MTT-S Int. Microw. Symp. Dig.*, Jun. 2019, pp. 1–3.

[6] J. C. Pedro, P. M. Cabral, T. R. Cunha, and P. M. Lavrador, "A multiple time-scale power amplifier behavioral model for linearity and efficiency calculations," *IEEE Trans. Microw. Theory Techn.*, vol. 61, no. 1, pp. 606–615, Jan. 2013.

[7] N. B. De Carvalho and J. C. Pedro, "Multitone frequency-domain simulation of nonlinear circuits in large- and small-signal regimes," *IEEE Trans. Microw. Theory Techn.*, vol. 46, no. 12, pp. 2016–2024, 1998.

[8] F. L. Ogboi *et al.*, "High bandwidth investigations of a baseband linearization approach formulated in the envelope domain under modulated stimulus," in *Proc. 44th Eur. Microw. Conf.*, Oct. 2014, pp. 361–364.

[9] T. Cappello, A. Duh, T. W. Barton, and Z. Popovic, "A dual-band dual-output power amplifier for carrier aggregation," *IEEE Trans. Microw. Theory Techn.*, vol. 67, no. 7, pp. 3134–3146, Jul. 2019.

[10] A. Santarelli *et al.*, "A double-pulse technique for the dynamic I/V characterization of GaN FETs," *IEEE Microw. Wireless Compon. Lett.*, vol. 24, no. 2, pp. 132–134, Feb. 2014.

[11] S. Bensmida *et al.*, "Power amplifier memory-less pre-distortion for 3GPP LTE application," in *Proc. Eur. Microw. Conf. (EuMC)*, Sep./Oct. 2009, pp. 1433–1436.

[12] G. P. Gibiino, F. F. Tafuri, T. S. Nielsen, D. Schreurs, and A. Santarelli, "Pulsed NVNA measurements for dynamic characterization of RF PAs," in *Proc. IEEE Int. Microw. RF Conf. (IMaRC)*, Dec. 2014, pp. 92–95.

[13] F. Meyer, private communication, May 2019.

[14] A. Technologies, *LTE and the Evolution to 4G Wireless*. Hoboken, NJ, USA: Wiley, 2009.

[15] S. Wei, D. L. Goeckel, and P. A. Kelly, "Convergence of the complex envelope of bandlimited OFDM signals," *IEEE Trans. Inf. Theory*, vol. 56, no. 10, pp. 4893–4904, Oct. 2010.

[16] H. Ochiai and H. Imai, "On the distribution of the peak-to-average power ratio in OFDM signals," *IEEE Trans. Commun.*, vol. 49, no. 2, pp. 282–289, Feb. 2001.